# Estimating forest parameters from top of atmosphere multi-angular radiance data using coupled radiative transfer models

Valérie C.E. Laurent[1], Wout Verhoef[2], Jan G.P.W. Clevers[1], Michael E. Schaepman[3],
[1] Centre for Geo-Information, Wageningen University, the Netherlands
[2] Faculty of Geo-Information Science and Earth Observation (ITC), University of Twente, the Netherlands
[3] Remote Sensing Laboratories, University of Zurich, Switzerland
valerie.laurent@wur.nl, verhoef@itc.nl, jan.clevers@wur.nl, michael.schaepman@geo.uzh.ch

ABSTRACT – *Traditionally, the estimation of forest parameters using physically-based canopy radiative transfer models (RT) requires correcting the remote sensing data to top-of-canopy (TOC) level by inverting an atmosphere RT model. By coupling the same canopy and atmosphere models, it is possible to simulate the top-of-atmosphere (TOA) radiance and to work directly with the measured TOA radiance data, thus avoiding the correction to TOC level. Many studies discussed the increased potential of multiangular data for parameter estimation, especially for forests, which have strong directional properties. These studies, however, were based on TOC data. In this study, we investigate the potential of multiangular data at TOA level, based on a case study for three Norway spruce stands in the Czech Republic, using multi-angular CHRIS data and the coupled SLC-MODTRAN model. The coupled model provided satisfactory TOA simulations of spectral and angular signatures, and the dimensionality of the parameter estimation problem increased with increasing angular sampling. Canopy cover, fraction of brown material, leaf chlorophyll and leaf dry matter content were estimated using all possible angular combinations. No combination was best for all parameters.*

## 1 INTRODUCTION

Traditionally, the estimation of forest parameters requires correcting the remote sensing data to top-of-canopy (TOC) level. This requires inverting an atmosphere radiative transfer (RT) model, which adds errors to the data that will be used for the inversion of the canopy RT model. By coupling the same canopy and atmosphere models, it is possible to simulate the top-of-atmosphere (TOA) radiance and to work directly with the measured TOA radiance data, thus avoiding the correction to TOC level. Many studies discussed the increased potential of multiangular data for parameter estimation (Kempeneers et al., 2008; Weiss et al., 2000), especially for forests (Huber et al., 2010), which have strong directional properties. These studies, however, were based on TOC data. This study coupled the SLC soil-leaf-canopy (Verhoef and Bach 2007) and the MODTRAN4 atmosphere (Berk et al., 2003) radiative transfer models to estimate forest parameters from multi-angular TOA radiance data. The study focused on three Norway spruce stands in the Czech Republic.

## 2 MATERIALS AND METHODS

### 2.1 Study area and data

The study area is located in a rather flat area in Eastern Czech Republic, at the Bily Kriz experimental research site in the Moravian-Silesian Beskydy Mountains, (18.54°E, 49.50°N; altitude 936 m above sea level). A detailed description of the environmental conditions can be found in (Kratochvilová et al., 1989). The forest area is dominated by montane Norway spruce (*Picea abies* (L.) Karst.). Three stands of different ages and structures were selected for the study (Table 1): YOUNG, OLD1 and OLD2. The data were collected in the first half of September 2006.

A set of multi-angular data was acquired on September 12$^{th}$, 2006, by CHRIS (Compact High Resolution Imaging Spectrometer) on board of the PROBA (Project for On Board Autonomy) satellite platform. Only four images covered the study area. Their acquisition geometry is shown in Figure 1. The images were acquired in chlorophyll mode (mode 4), resulting in 18 spectral bands in the range 485-802 nm at a spatial resolution of 17 m. The images were radiometrically calibrated by the data provider and were further de-striped, geo-corrected and ortho-rectified using nearest neighbor interpolation. Band 15, centered at 761 nm, was not used because it sampled one of the oxygen absorption features and was very noisy. An AISA (Airborne Imaging Spectro-radiometer) Eagle image with 40 cm pixel size was acquired on September 14$^{th}$, 2006. It was atmospherically corrected using ATCOR4.

The plant area index (PAI), defined as half of the total plant area (needles and non photosynthetic plant material) per unit of ground surface area (Chen, 1996),

Table 1. Stand characteristics and model inputs (DBH: diameter at breast height, LIDF: leaf inclination distribution function, Sph: spherical).

| Stand | | YOUNG | OLD1 | OLD2 |
|---|---|---|---|---|
| Age (years) | | 29 | 100 | 75 |
| Density (trees/ha) | | 1450 | 160 | 420 |
| DBH (cm) | | 14 | 53 | 37 |
| Canopy | PAI | 8.88 | 5.73 | 7.35 |
| | fB | 0.13 | 0.23 | 0.4 |
| | D | 0 | 0 | 0 |
| | Hot | 0.01 | 0.01 | 0.01 |
| | LIDF | Sph | Sph | Sph |
| | Cv | 0.9 | 0.55 | 0.7 |
| | Zeta | 0.34 | 0.24 | 0.26 |
| Needle | Cab (µg/cm$^2$) | 55 | 60 | 65 |
| | Cw (cm) | 0.02 | 0.02 | 0.02 |
| | Cdm (g/cm$^2$) | 0.04 | 0.04 | 0.04 |
| | Cs | 0 | 0 | 0 |
| | N | 2.7 | 2.5 | 2.3 |
| Bark | Cab (µg/cm$^2$) | 10 | | |
| | Cw (cm) | 0 | | |
| | Cdm (g/cm$^2$) | 0.5 | | |
| | Cs | 15 | | |
| | N | 10 | | |

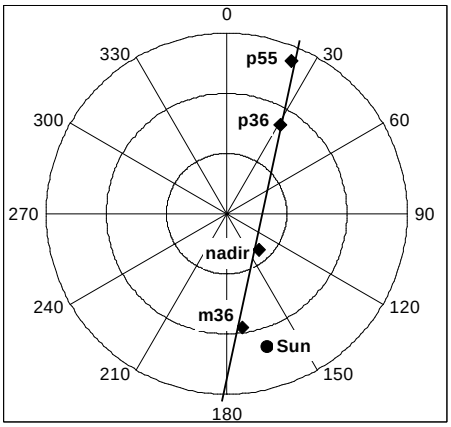


Figure 1: Polar view of the geometry of the CHRIS acquisition.

was estimated in each stand by three methods: LAI-2000 plant canopy analyzer, hemispherical photograph, and TRAC (Tracing Radiation and Architecture of Canopies) (Homolová et al., 2007). The obtained values were averaged to one PAI value for each stand. The crown cover (Cv) was estimated by classifying the AISA image (Lukeš, 2009).

Ten sample trees in the YOUNG stand and 20 in the OLD1 stand were selected for canopy and needle measurements. Only canopy measurements were made in the OLD2 stand. Canopy structure measurements included tree height, crown radius, and crown length.

The spectral properties of the main background components (soil, humus, litter, understory species) and of the bark were measured in the field at 1 nm resolution with an ASD spectro-radiometer.

## 2.2 Radiative transfer models

The Soil-Leaf-Canopy (SLC) model was used to simulate the four top-of-canopy (TOC) reflectance components of the stands. It couples:

a) 4SOIL: soil reflectance model which was not used in this study,

b) PROSPECT: leaf optical properties model (Jacquemoud and Baret, 1990), modified to include brown pigments (Cs) (Verhoef and Bach, 2003),

c) 4SAIL2: canopy reflectance model which includes the crown clumping effect thanks to the introduction of two additional inputs: crown cover (Cv) and tree shape factor (Zeta) defined as the crown diameter divided by the height of the crown centre above ground (Verhoef and Bach, 2007). 4SAIL2 also allows mixing green and brown leaves in the canopy by using the fraction of brown material (fB) and the dissociation factor (D). The brown leaves were used for the bark.

The MODTRAN4 model was used for the atmosphere. The following options were selected: DISORT algorithm with 8 streams, medium speed correlated-k option with 17 values, and 5 cm$^{-1}$ database.

## 2.3 Calculation of the TOA radiance

The 4-stream RT theory provides a simple but accurate framework for radiative transfer modeling. We use subscripts to indicate the direction of the radiation: *s* for the sun direction, *o* for the observer direction and *d* for diffuse hemispherical radiation. When ignoring the adjacency effect, the TOA radiance $L_o$ can be calculated as (Laurent et al., Submitted):

$$L_o = L_{atm} + \frac{G_{ssdo} r_{sd} + G_{sddo} r_{dd}}{1 - r_{dd}\rho_{dd}} + \frac{G_{sdoo} + G_{mult} r_{sd}}{1 - r_{dd}\rho_{dd}} r_{do} + G_{ssoo} r_{so}, \quad (1)$$

where $L_{atm}$ is the atmospheric path radiance, the *r* terms are the reflectance factors of the canopy, $\rho_{dd}$ is the spherical albedo of the atmosphere, and the *G* terms are atmospheric gain factors for the double pass in the atmosphere. The *G* factors were calculated from the total path radiance, the sunlight ground-reflected radiance, and the total ground-reflected radiance outputs of three MODTRAN runs for Lambertian surfaces (Laurent et al., Submitted). Canopy reflectances and *G* factors were resampled to the

CHRIS bands using Gaussian approximations of the sensor response functions.

### 2.4 Model parameterization

The background signature was calculated as the average of the signatures of the background components, weighted by their fractional area. The PROSPECT model was used to simulate the optical properties of the needles and bark material. It was not designed for that, so it was optimized to match the measured bark signature, and the parameters for the needles were tuned using the four angular measurements at TOA level, together with the D parameter (Table 1).

The same atmospheric properties were used for the four images. The urban aerosol type was chosen in MODTRAN because of the dominant north wind blowing from an industrial zone and high air concentration of $SO_2$. The visibility was chosen as the smallest value (100 km) for which the simulated $L_{atm}$ was smaller than all radiances in all CHRIS images.

### 2.5 Local sensitivity analysis

A local sensitivity analysis (LSA) was performed based on the Jacobian values. For each observation direction $o$, the Jacobian matrix $\mathbf{J}_o$ is the matrix of the partial derivatives of the model output $L_o$ with respect to each input parameter $p_k$, normalized assuming a uniform distribution over its potential variation range:

$$\mathbf{J}_o = \left\lfloor j_{o,i,k} \right\rfloor_{1\le i\le n_b,\ 1\le k\le n_p},$$
$$\text{with } j_{o,i,k} = \frac{\partial L_o(\theta_o, \lambda_i)}{\partial p_k}, \qquad (2)$$

where $n_b$ is the number of bands and $n_p$ is the number of parameters. The hotspot parameter (hot) was changed by 0.005 because of its very small value.

We note $\Theta$ the ensemble of the observation directions used in the multi-angular analysis. The Jacobian matrices for $o$ in $\Theta$ were vertically stacked into the matrix **J**.

Only the most influent parameters can be estimated. To evaluate the influence of each parameter, the indicator $\alpha_k$ was defined as:

$$\alpha_k = \sqrt{\frac{\sum_{o\in\Theta}\sum_{i=1}^{n_b} w_i j_{o,i,k}^2}{\sum_{o\in\Theta}\sum_{i=1}^{n} w_i}}, \qquad (3)$$

where the $w$ terms are the weights that were introduced to account for the irregular spectral distance of the CHRIS bands:

$$\begin{cases} w_1 = (\lambda_2 - \lambda_1) \\ w_i = (\lambda_{i+1} - \lambda_{i-1})/2, \ 2 \le i \le n-1 \\ w_n = (\lambda_n - \lambda_{n-1}) \end{cases}. \qquad (4)$$

To allow easier comparison between stands, the $\alpha$ values were normalized ($\alpha_{norm}$).

A Singular Value Decomposition (SVD) was then applied to **J**, yielding the singular matrix **S**. **S** relates the transformed output differences $\mathbf{U}^T\Delta\mathbf{L}$ to the transformed parameter variations $\mathbf{V}^T\Delta\mathbf{p}$ as:

$$\mathbf{U}^T\Delta\mathbf{L} = \mathbf{S}\mathbf{V}^T\Delta\mathbf{p}, \qquad (5)$$

where $\Delta\mathbf{L}$ is the stacked vector of model output differences for $o$ in $\Theta$ and $\Delta\mathbf{p}$ is the vector of normalized parameter variations. Because **S** is diagonal and $\mathbf{U}^T$ and $\mathbf{V}^T$ are orthonormal, there is a one-to-one relationship between $\Delta\mathbf{L}$ and $\Delta\mathbf{p}$. Therefore, the rank of **S** is the dimensionality of the estimation problem. The rank of **S** was taken as the number of singular values needed to reach 95% of the sum of all singular values.

### 2.5 Parameter estimation

The cost function $\chi$ was defined using the same structure as the $\alpha$ indicator:

$$\chi = \sqrt{\frac{\sum_{o\in\Theta}\sum_{i=1}^{n_b} w_i (\Delta L_o(\lambda_i))^2}{\sum_{o\in\Theta}\sum_{i=1}^{n} w_i}}. \qquad (6)$$

The look-up table (LUT) method was chosen because of its ability to find the global minimum of the cost function. The free parameters in the LUT were chosen based on the results of the LSA.

## 3 RESULTS AND DISCUSSION

### 3.1 Simulations

The TOA simulations were satisfactory. The $\chi$ values for $\Theta$ = {m36, nadir, p36, p55} were: 5.9 mW/(m$^2$.sr.nm) for the YOUNG stand, 9.5 for the OLD1 stand, and 7.6 for the OLD2 stand.

Figure 2 presents the spectral simulation results for the YOUNG stand. The monoangular $\chi$ values were smaller in the forward than in the backward direction ($\Theta_{nadir}$ = -16°). The signatures were overestimated in the nadir, p36, and p55 directions and underestimated in the m36 direction. This might be due to the leaf angle distribution function or to the

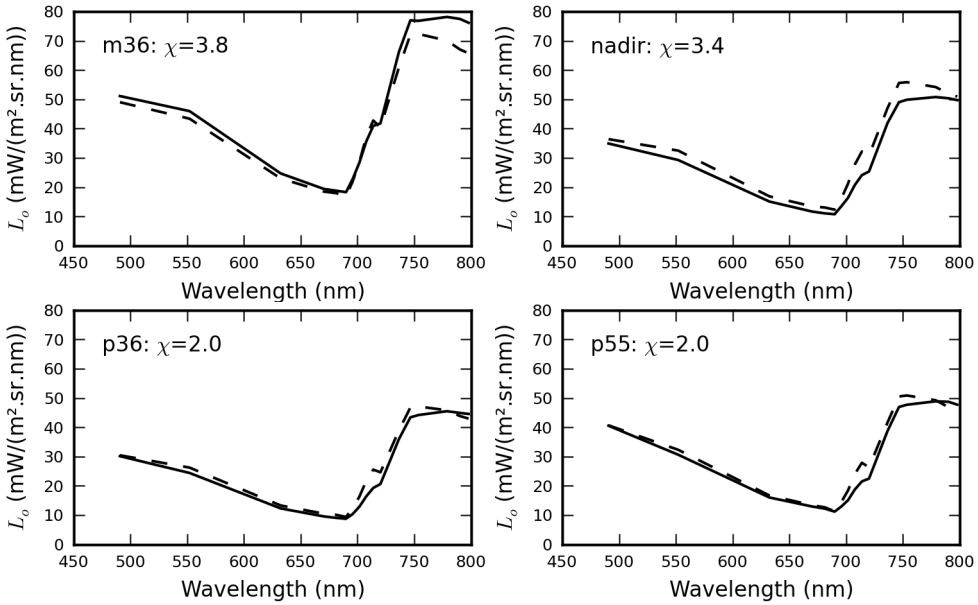


Figure 2. Spectral simulations (dashed lines) and CHRIS measurements (solid lines) of the TOA radiance for the four available images for the YOUNG stand

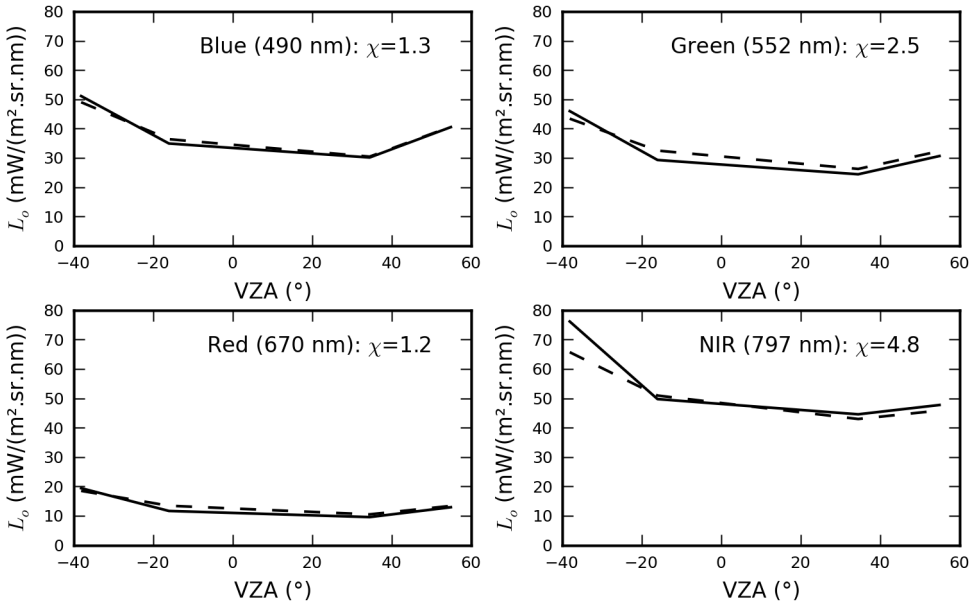


Figure 2. Angular simulations (dashed lines) and CHRIS measurements (solid lines) of the TOA radiance for four selected wavelengths for the YOUNG stand

assumption of constant atmospheric parameters for the four angles.

The angular results for the YOUNG stand are shown in Figure 3. Both the simulations and the measurements present the bowl shape expected for dense coniferous forests (Verrelst et al., In press). The $\chi$ values were smallest in the visible domain, especially in the blue and red band where the radiance is lowest, and larger in the NIR band, where the radiance is highest. This may be due to the atmospheric path radiance which is most important in the visible and accounts for the most part of the

radiance, with only a small part coming from the canopy. Thus, inaccuracies in the canopy reflectance were less important in the visible domain. On the contrary, the atmospheric path radiance is very small in the NIR domain, and inaccuracies at the canopy level fully translated to TOA level.

Similar trends were observed for the OLD1 and OLD2 stands, but with higher $\chi$ values. This may be due to the lesser quality of the field data for these stands.

### 3.2 Local sensitivity analysis

For each angular combination, the $\alpha_{norm}$ values were averaged over the three stands (not shown). All combinations presented similar influence profiles, except for the hotspot parameter. Hot was most influent for m36 ($\alpha_{norm}$ = 0.33) and nadir (0.14) and was not influent for the forward angles (<0.04). For the multiangular combinations, its influence depends on which angles were used (e.g: 0.22 for four angles). For the other parameters, the most influent were fB (0.18-0.22), Cv (0.14-0.22), needleCdm(0.14-0.17), LIDFa (0.09-0.17), and needleCab (0.06-0.08).The bark ($\alpha_{norm}$ < 0.03) and atmosphere ($\alpha_{norm}$ < 0.04) parameters were least influent.

The importance of the hotspot parameter is due to the wide angular area of influence caused by the very high PAI of the three stands. The m36 image is close to the hotspot, and the nadir image is close to the principal plane (relative azimuth = 25°). The value of 0.01 for forests is well known. The LIDFa parameter was also very influent, but for coniferous stands, we cannot assume any other leaf distribution than spherical.

The local dimensionality values obtained from the SVD are presented in Table 2. For each combination, the three stands had very similar values, with the YOUNG stand having slightly smaller dimensionality. The dimensionality increases when using more angles in the combination, thus showing the increasing information content when increasing the angular sampling.

Table 2. Dimensionality

| | YOUNG | OLD1 | OLD2 |
|---|---|---|---|
| nadir | 3 | 3 | 3 |
| m36 | 3 | 3 | 3 |
| p36 | 3 | 3 | 3 |
| p55 | 4 | 4 | 4 |
| nadir_m36 | 4 | 4 | 4 |
| nadir_p36 | 4 | 5 | 5 |
| nadir_p55 | 5 | 5 | 5 |
| m36_p36 | 4 | 4 | 4 |
| m36_p55 | 4 | 5 | 5 |
| p36_p55 | 5 | 5 | 5 |
| nadir_m36_p36 | 5 | 5 | 5 |
| nadir_m36_p55 | 5 | 6 | 6 |
| nadir_p36_p55 | 5 | 6 | 6 |
| m36_p36_p55 | 5 | 6 | 6 |
| 4 angles | 5 | 6 | 6 |

### 3.3 Parameter estimation

Based on the dimensionality results, it was decided to have four free parameters in the LUT. The four parameters which were most influent and also most relevant for applications (forest health, fuel moisture, carbon stock…) were used: fB, Cv, needleCdm, and needleCab. fB and Cv were sampled from 0 to 1 in steps of 0.1, Cab from 0 to 100 in steps of 5, and Cdm from 0 to 0.05 in steps of 0.005.

The estimation results for the YOUNG stand are presented in Table 3. In all cases, only one solution was found in the LUT. No combination provided the best estimates for all parameters. Some combinations, however, were able to provide good estimates for two parameters. The best estimates for Cv were obtained

Table 3. Parameter estimates for the YOUNG stand (best estimates in bold).

| | Cv | fB | Cab (g/cm$^2$) | Cdm (g/cm$^2$) | $\chi$ | # solutions |
|---|---|---|---|---|---|---|
| nadir | 0.8 | 0.0 | 75 | 0.050 | 1.044 | 1 |
| m36 | 1.0 | 0.2 | 50 | 0.025 | 1.672 | 1 |
| p36 | **0.9** | **0.1** | 75 | 0.045 | 0.960 | 1 |
| p55 | 0.8 | 0.2 | 75 | 0.030 | 0.982 | 1 |
| nadir_m36 | 0.6 | 0.0 | **55** | 0.025 | 1.689 | 1 |
| nadir_p36 | 0.7 | 0.0 | 75 | **0.040** | 0.722 | 1 |
| nadir_p55 | 0.8 | **0.1** | 75 | **0.040** | 0.762 | 1 |
| m36_p36 | 0.7 | 0.2 | 50 | 0.015 | 1.673 | 1 |
| m36_p55 | 1.0 | 0.4 | 50 | 0.005 | 1.749 | 1 |
| p36_p55 | **0.9** | **0.1** | 75 | 0.045 | 0.710 | 1 |
| nadir_m36_p36 | 0.7 | 0.0 | 60 | 0.035 | 1.377 | 1 |
| nadir_m36_p55 | 0.8 | 0.2 | 60 | 0.025 | 1.620 | 1 |
| nadir_p36_p55 | 0.8 | **0.1** | 75 | **0.040** | 0.618 | 1 |
| m36_p36_p55 | **0.9** | 0.4 | **55** | 0.005 | 1.469 | 1 |
| 4 angles | 0.8 | 0.2 | 60 | 0.025 | 1.270 | 1 |

by combinations including p36, best estimates for Cab using m36 and best estimates for Cdm using nadir, and the best estimates of fB used only nadir and forward angles, similar to Cdm. The m36 angle was only used for the Cv and Cab estimates. It is interesting to note that the nadir angle was not used in the combinations providing the best Cv and that the combination using the four angles did not provide the best estimate for any parameter.

The results for the OLD1 and OLD2 stands were different, but similarly to the YOUNG stand, it was not possible to distinguish a single combination providing the best estimates.

## 5 CONCLUSION

The coupled SLC-MODTRAN model was able to provide satisfactory simulations of the TOA radiance of the coniferous stands. Despite the simplicity of SLC, the brown material and crown clumping features adequately mimicked the stand structures, also when seen from multiple observation directions.

The SVD is a very interesting tool to assess the dimensionality of the estimation problem and to get insight in the influence of the parameters, thus being of great interest for steering the inversion process. The multiangular SVD proved that the dimensionality increases with increasing number of angles at TOA level. In the future, the LUT will be extended to more parameters to make full use of the extra information provided by the multiangular data.

## 6 ACKNOWLEDGEMENT

The data collection was conducted under ESA/PECS project No. 98029 and provided by the Institute of Systems Biology and Ecology, Academy of Sciences of the Czech Republic. The authors wish to thank Petr Lukeš and Lucie Homolová for their help with the data and Allard de Wit for his assistance with model implementation and LUTs.

## 7 REFERENCES

Berk, A., Anderson, G.P., Acharya, P.K., Hoke, M.L., Chetwynd, J.H., Bernstein, L.S., Shettle, E.P., Matthew, M.W., and Adler-Golden, S.M. 2003, MODTRAN4 Version 3 Revision 1 User's manual. (p. 97): Airforce Research Laboratory, Hanscom, MA, USA.

Chen, J.M., 1996, Optically-based methods for measuring seasonal variation of leaf area index in boreal conifer stands. *Agricultural and Forest Meteorology, 80*, 135-163.

Homolová, L., Malenovský, Z., Hanuš, J., Tomášková, I., Dvořáková, M., and Pokorný, R., 2007, Comparison of different ground techniques to map leaf area index of Norway spruce forest canopy. In M.E. Schaepman, S. Liang, N.E. Groot & M. Kneubühler (Eds.), *10th ISPMSRS*. Davos, Switzerland: Intl. Archives of the Photogrammetry, Remote Sensing and Spatial Information Sciences.

Huber, S., Koetz, B., Psomas, A., Kneubühler, M., Schopfer, J., Itten, K., and Zimmermann, N.E., 2010, Impact of multiangular information on empirical models to estimate canopy nitrogen concentration in mixed forest. *Journal of Applied Remote Sensing, 4*

Jacquemoud, S., and Baret, F., 1990, PROSPECT: A model of leaf optical properties spectra. *Remote Sensing of Environment, 34*, 75-91.

Kempeneers, P., Zarco-Tejada, P.J., North, P.R.J., de Backer, S., Delalieux, S., Sepulcre-Canto, G., Morales, F., van Aardt, J.A.N., Sagardoy, R., Coppin, P., and Scheunders, P., 2008, Model inversion for chlorophyll estimation in open canopies from hyperspectral imagery. *International Journal of Remote Sensing, 29*, 5093-5111.

Kratochvilová, I., Janouš, D., Marek, M., Barták, M., and Řiha, L., 1989, Production activity of mountain cultivated Norway spruce stands under the impact of air pollution. I. General description of problems. *Ekológia, 8*, 407-419.

Laurent, V.C.E., Verhoef, W., Clevers, J.G.P.W., and Schaepman, M., Submitted, Estimating forest parameters from top-of-atmosphere radiance satellite measurements using coupled radiative transfer models. *Remote Sensing of Environment*

Lukeš, P., 2009, Retrieval of canopy cover of the Norway spruce stands in the Bily Kriz area (CZ) from classification of AISA Eagle data. Personal communication.

Verhoef, W., and Bach, H., 2003, Simulation of hyperspectral and directional radiance images using coupled biophysical and atmospheric radiative transfer models. *Remote Sensing of Environment, 87*, 23-41.

Verhoef, W., and Bach, H., 2007, Coupled soil-leaf-canopy and atmosphere radiative transfer modeling to simulate hyperspectral multi-angular surface reflectance and TOA radiance data. *Remote Sensing of Environment, 109*, 166-182.

Verrelst, J., Clevers, J.G.P.W., and Schaepman, M.E., In press, Merging the Minnaert- k Parameter With Spectral Unmixing to Map Forest Heterogeneity With CHRIS/PROBA Data. *IEEE Transactions on Geoscience and Remote Sensing*

Weiss, M., Baret, F., Myneni, R.B., Pragnère, A., and Knyazikhin, Y., 2000, Investigation of a model inversion technique to estimate canopy biophysical variables from spectral and directional reflectance data. *Agronomie, 20*, 3-22.